BJR

https://doi.org/10.1259/bjr.20180695

Received: 07 August 2018 | Revised: 20 December 2018 | Accepted: 20 December 2018

Cite this article as:
Kaya F, Ufuk F, Karabulut N. Diagnostic performance of contrast-enhanced and unenhanced combined pulmonary artery MRI and magnetic resonance venography techniques in the diagnosis of venous thromboembolism. *Br J Radiol* 2019; **92**: 20180695.

FULL PAPER

Diagnostic performance of contrast-enhanced and unenhanced combined pulmonary artery MRI and magnetic resonance venography techniques in the diagnosis of venous thromboembolism

[1]FURKAN KAYA, [2]FURKAN UFUK and [3]NEVZAT KARABULUT

[1]Department of Radiology, Afyonkarahisar Health Sciences University, Afyonkarahisar, Turkey
[2]Department of Radiology, Pamukkale University School of Medicine, Kinikli, Denizli, Turkey
[3]Department of Radiology, Tekden Hospital, Denizli, Turkey

Address correspondence to: Dr Furkan Ufuk
E-mail: *furkan.ufuk@hotmail.com*

Objective: We aimed to determine the diagnostic performance of the contrast-enhanced and unenhanced combined pulmonary arterial MRI and magnetic resonance venography techniques in the diagnosis of venous thromboembolism (VTE).
Methods: 44 patients who underwent CT pulmonary angiography (CTPA) for suspected PE constituted the study population. Patients underwent combined pulmonary and lower extremity MRI, and Doppler ultrasonography within 72 h after CTPA. Combined MRI included two sequences: unenhanced steady-state free precession (SSFP) and contrast-enhanced three-dimensional (3D) gradient echo (GRE). The presence of emboli in pulmonary arteries and thrombi in lower extremity veins on 3D-GRE and SSFP sequences was recorded.
Results: CTPA showed a total of 244 emboli in 33 (75%) patients whereas contrast-enhanced 3D-GRE MRI showed deep vein thrombosis (DVT) in 34 (77%) subjects. Sensitivities for SSFP *vs* 3D-GRE MRI respectively in PE detection were 87.9 *vs* 100% on a per-patient basis, and 53.7 *vs* 73% on a per-embolus basis. Of 34 patients with established DVT, 31 (91%) were detected by Doppler ultrasound and 29 (85%) were detected by SSFP technique respectively.
Conclusion: Both contrast-enhanced and unenhanced combined MRI of acute PE and DVT are feasible one-stop-shopping techniques in patients with suspected thromboembolism.
Advances in knowledge: Pulmonary VTE is a common disease with high mortality. Non-invasive techniques withhigh accuracy are required for the assessment of VTE. CT-related radiation and contrast material risks cause concerns. MRI is a radiation-free technique evaluating the vessels with and without contrast. Combined contrast enhancedor unenhanced pulmonary and lower extremity MRI is feasible in patients with suspected thromboembolism.

INTRODUCTION

Pulmonary embolism (PE) is a common disorder with high mortality and usually results from deep vein thrombosis (DVT) of lower extremities.[1] Although they represent different aspects of the same process, PE and DVT are generally evaluated with different imaging methods. In current clinical practice, CT pulmonary angiography (CTPA) is used as the first line imaging modality in PE diagnosis, whereas Doppler ultrasonography is the initial modality in the diagnosis of DVT.[2–4] A single reliable test that can accurately assess both pulmonary and lower extremity vasculature and concretely show the presence or absence of a clot is highly desirable. For this purpose, combined pulmonary CTPA and indirect CT venography has been introduced as a one-stop-shop imaging technique for venous thromboembolism (VTE). However, the technique is not applied on routine basis due to concerns of increased radiation dose.[5]

Pulmonary MRI has become feasible with the advent of fast acquisition techniques. MRI is particularly useful in patients with suspected PE who have contraindications for CT scanning (*i.e.* pregnancy, allergy to iodine-containing contrast medium), or in those in whom radiation exposure is a major concern.[6] Comprehensive MRI of VTE can be achieved by combined pulmonary and lower extremity MRI with or without use of contrast medium. Unenhanced imaging of pulmonary arteries (PAs) and

deep veins can be obtained using steady-state free precession (SSFP) technique whereas 3-dimensional T_1 weighted gradient echo sequence (3D-GRE) is used for contrast-enhanced pulmonary MRI and indirect MR venography (MRV).[6–8] Kluge et al[9] reported that combined MRI examinations consisting of pulmonary MRI for suspected PE and indirect contrast-enhanced MR venography for DVT is a routinely feasible technique for the diagnosis of VTE.

The purpose of this study was to evaluate the diagnostic performances of contrast enhanced and unenhanced combined pulmonary and lower extremity MRI sequences in the diagnosis of pulmonary embolism and deep vein thrombosis in patients with suspected venous thromboembolism.

METHODS AND MATERIALS

Study group

This prospective HIPAA-compliant study was approved by the local ethics committee. The study population was recruited from 529 patients who had undergone CTPA for suspected pulmonary embolism. Before CTPA, patients were asked whether they wanted to participate in this study. Patients who agreed to undergo combined MRI (PA MRI and MRV) after CTPA constituted the study group. Patients with contraindications for MRI, those who were uncooperative or who had MRI incompatible implants, those with claustrophobia or history of gadolinium based contrast medium allergy, those with an estimated glomerular filtration rate (eGFR) of ≤60 ml min^{-1} 1.73 m^2, and those with a duration of >72 h between CTPA and MRI were not included. The final study group consisted of 44 patients (33 male, 11 female; mean age, 52.1 ± 15.3 years; range, 23–83 years) who met the inclusion criteria and gave written informed consent.

CT pulmonary angiography

CT imaging was performed using a 16-detector row CT scanner (Brilliance 16, Philips Medical Systems, Best, Netherlands) during suspended shallow inspiration. The scanning parameters were as follows: tube voltage, 120 kV; tube current, 100 mAs; collimation, 16 × 0.75 mm; field of view, 300 mm; matrix, 512 × 512; rotation time, 0.75 s; table speed, 15 mms^{-1} and beam pitch, 0.94. We administered 75–80 ml of iopromide (Ultravist 370 mg I ml^{-1}, Bayer HealthCare) from the antecubital vein at a rate of 4 ml s^{-1}. The raw data were reconstructed as 3 mm thick transverse sections with 1.5 mm reconstruction intervals, and all images were transferred to the workstation (Extended Brilliance Workspace, Philips Medical Systems).

Doppler ultrasonography

Lower extremity Doppler ultrasonography imaging was performed before MRI. The sonographic imaging was performed prospectively by a radiologist, who was unaware of the CTPA results, using a high-resolution Doppler ultrasonography device (Logic E9, GE Medical Systems) equipped with 6–12 MHz matrix linear and 2–6 MHz broadband convex probes. Bilateral pelvic, thigh and leg veins were imaged using appropriate transducers according to the site of evaluation. The patency of veins, presence of any filling defect and response to augmentation were evaluated. Direct observation of the thrombus on Doppler ultrasonography, lack of flow in the venous structures, increase in vessel diameter, non-compressibility, and the absence of response to augmentation were used as the diagnostic criteria for DVT.

Pulmonary MRI

MRI was performed using 1.5 T superconductive magnet (Signa Excite HD, GE Medical Systems) and 8-channel phased-array torso coil positioned over the anterior and posterior chest. The maximum gradient strength was 33 mT/m and the slew rate was 120 mT m^{-1} s^{-1}. The field of view was set to 40 × 32 cm to include the area between the thoracic inlet and the crura of the diaphragm while the patient in the supine position with arms along both sides. Fat-suppressed unenhanced SSFP images were obtained using the "fast imaging employing steady-state acquisition" (fast imaging employing steady-state acquisition sequence) during breath-hold at expiration or free breathing according to clinical condition of the subjects. Then, fat-suppressed breath-hold T1A images were obtained in the transverse plane using three-dimensional gradient echo (3D-GRE) sequence (liver acquisition with volume acceleration), before and after i.v. injection of 0.1 mmol kg^{-1} Gadobutrol (Gadovist, Bayer HealthCare). The contrast injection rate was 2 ml s^{-1}, which was followed by the i.v. administration of 20 ml of saline flush at the same rate. The transverse fat-suppressed 3D-GRE sections were obtained 20–30 s following the contrast injection. The MRI parameters are presented in Table 1.

Lower extremity magnetic resonance venography

MRV examination was performed following the pulmonary MRI by moving the torso coil to the lower extremity in two steps with 5 cm overlap between two stations. The first station covered the area from the level of the iliac crest to the mid-thigh followed by the second station which covered 5 cm distal of the popliteal fossa. Indirect MRV images were performed using axial SSFP followed by axial and coronal 3D-GRE, 4–5 min after the injection of contrast media. The imaging parameters were the same as chest MRI except for thicker slices (5 mm for 3D-GRE and 10

Table 1. The imaging parameters in pulmonary artery MRI lower extremity MRV sequences

Sequences	TR/TE (ms)	Flip Angle	NEX	Matrix	Slice thickness/gap[a] (mm)	Parallel imaging factor
SSFP	4.2/1.8	70°	2	288 × 160	5/1.5	–
3D-GRE	4.4/2.1	12°	0.75	320/192	3/0	2

3D-GRE, three dimensional gradient echo; MRV, magnetic resonance venography; NEX, number of excitations; SSFP, steady-state free precession.
[a]5/0 mm for 3D-GRE and 10/2.5 for SSFP in MRV.

Figure 1. A 73-year-old man with chest pain. (a), Axial CTPA at level of left atrium shows filling defects *(arrow)* in right lower lobe artery. There is also a pleural effusion on the right side *(arrowhead)*. Axial contrast enhanced 3D-GRE (c) and unenhanced SSFP (b) images at level of left atrium show emboli in right lower lobe artery *(arrows)* and pleural effusion on the right side *(arrowhead)*. Axial (d) and coronal (e) contrast enhanced 3D-GRE images show thrombi in left main iliac vein *(arrows)*. Axial unenhanced SSFP image (f) shows thrombi in left main iliac vein *(arrow)*. Doppler ultrasonography image (G) in axial plane shows hypoechoic thrombus in the left main iliac vein *(arrow)*. 3D-GRE, three-dimensional gradient echo; CTPA, CT pulmonary angiography; SSFP, steady-state-free-precession.

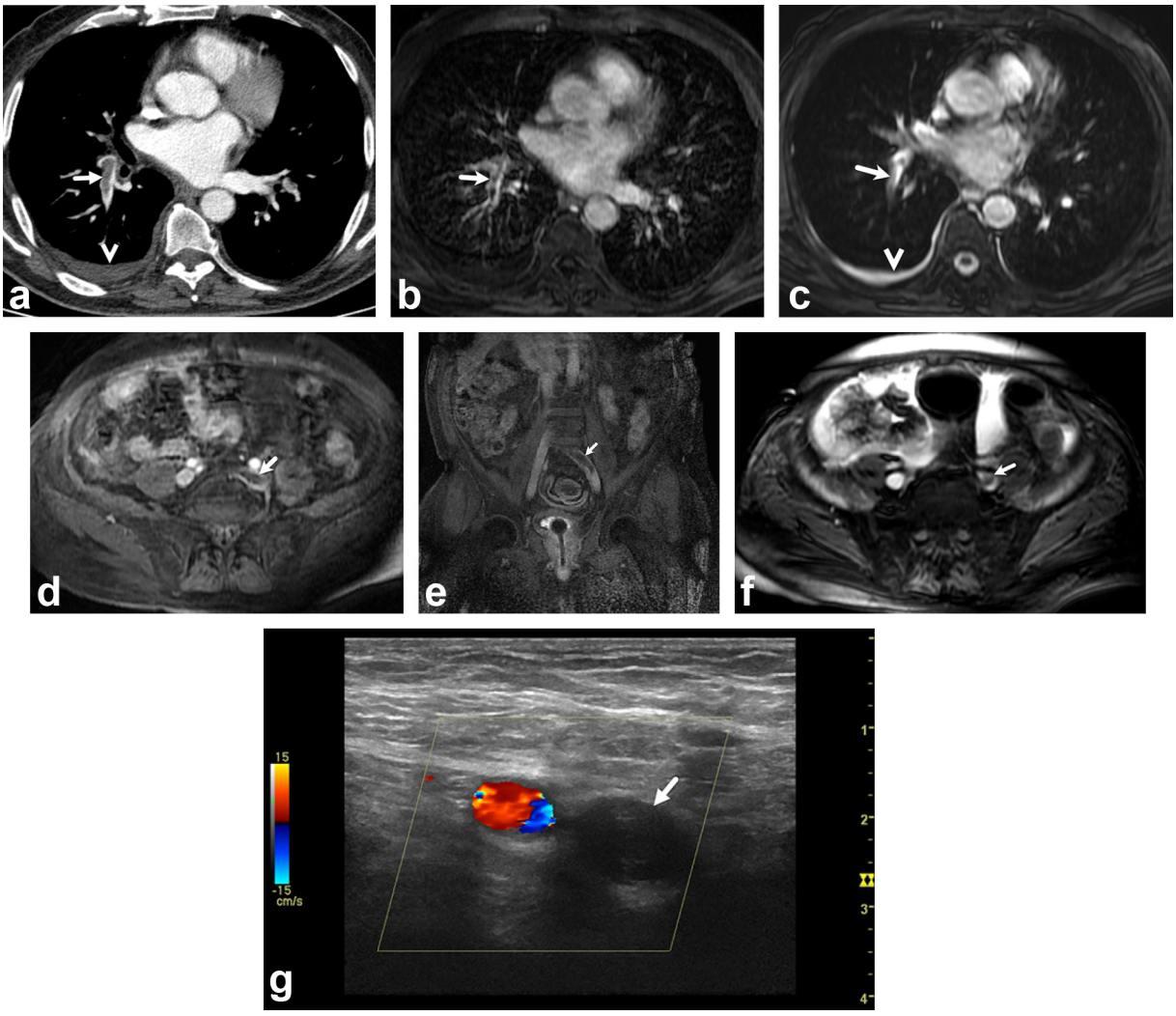

mm for SSFP) (Table 1). The parallel imaging technique [Array Spatial Sensitivity Encoding Technique (ASSET 2)] was used in 3D-GRE sequences during combined MRI (PA MRI and MRV) scanning.

Image interpretation

Images from CTPA, pulmonary arterial MRI and MRV images were retrospectively evaluated in two different sessions by a fellowship trained chest radiologist with a 16 year experience. The reader first evaluated CTPA images. Then, at least 30 days later, pulmonary arterial MRI and MRV images at the same session were evaluated without knowing the results of CTPA for the presence of PE. CTPA images were evaluated in both mediastinal (WW: 350, WL: 50) and parenchymal (WW: 1600, WL: −600) window settings.

Pulmonary MRI scans were consecutively evaluated (first SSFP, then 3D-GRE) without knowing the results of CTPA. First, the reader evaluated the image quality (insufficient contrast, visibility of pulmonary vessels) and artifacts on each sequence using a 2-point scale: "good" and "limited". Then, the presence and location of PE were recorded in the standard forms. The accompanying abnormalities in the lungs and the mediastinum were also recorded. For the anatomical location of the emboli, the main and lobar PAs were recorded in 10 different vascular structures (right and left main PAs, right and left upper lobe PAs, right interlobar PA, right middle lobe PA, right and left lower lobe PAs, left descending PA and lingular artery), and the segmental PAs were recorded in 18 different vascular structures according to the lung segments. The diagnosis of acute embolism on MRI scans was made according to

the presence of a central filling defect in the artery, complete filling defect or partial filling defect with an acute angle at least in two consecutive sections in the PAs on MRI. Using the CTPA as the gold-standard, the diagnostic accuracy of both MRI techniques were calculated.

The MRV sequences were evaluated in the same session with pulmonary MRI by the same observer who was blinded to Doppler ultrasonography results. As in pulmonary arterial MRI, the image quality of the sequences and the factors that influence the quality were initially recorded. The MRV image quality was evaluated on a 2-point scale, as "good" and "limited". Then, the MRV sequences were consecutively evaluated (first SSFP, then 3D-GRE) without knowing the Doppler US results and the presence and anatomical locations of DVT were recorded in the standard forms. Hypointense filling defects in the vein in consecutive sections at MRV sequences were accepted as the direct diagnostic criteria for DVT. For the anatomical locations DVT, the lower extremity veins were divided in 16 different venous segments: bilateral common iliac, external iliac, common femoral, superficial and deep femoral, popliteal veins and, great and lesser saphenous veins.

The gold-standards were CTPA in the diagnosis of PE, and contrast-enhanced 3D-GRE MRV in the diagnosis of DVT. The effectiveness of the combined MRI (pulmonary arterial MRI and MRV) sequences in the diagnosis of VTE was evaluated.

Statistical analysis

The data analysis was performed on a personal computer using a statistical software (SPSS 21 for Windows, Chicago, IL). Using CTPA as a gold-standard in the diagnosis of PE and the contrast-enhanced indirect MRV in the diagnosis of DVT, the sensitivity, specificity, positive predictive value (PPV), negative predictive value (NPV) and accuracy of SSFP and 3D-GRE sequences were calculated in pulmonary arterial MRI. Also, the diagnostic performance of the SSFP sequence and Doppler ultrasonography in the lower extremity MRV was calculated. The differences between imaging techniques in the dependent groups were evaluated using McNemar's test. The agreement of MRV sequences and Doppler ultrasonography was evaluated with the κ coefficient. A *p*-value less than 0.05 was considered statistically significant.

RESULTS

The mean period between CTPA and MRI scans was 26.6 ± 22.4 h (range: 1–72 h). Following CTPA, Doppler ultrasonography was performed within 10 h. The mean combined MRI (pulmonary arterial MRI and MRV) acquisition time was 19.09 ± 6.73 min. 33 (75%) of the 44 patients had PE on CTPA. Using 3D-GRE MRV, 34 (77%) patients were diagnosed with DVT. 27 (61%) patients had both PE and DVT (Figure 1); 6 (14%) patients had PE without DVT; 7 (15.9%) had DVT without PE; and 4 patients (9%) had neither emboli nor DVT.

Evaluation of PAs

The image quality of the pulmonary arterial MRI was rated as "limited" in 2% (n = 1) and 6.8% (n = 3) of subjects on SSFP and 3D-GRE techniques, respectively. A total of 244 emboli were detected in 33 (75%) patients on CTPA. There were 112 emboli in the common and lobar PAs whereas 132 emboli were detected at segmental level. Isolated segmental PE was detected in three (6.8%) patients. On per patient-basis, emboli were demonstrated in all 33 (100%) patients on contrast-enhanced 3D-GRE sequence whereas SSFP showed PE in 29 (87.9%) subjects. On per embolus-basis, 178 (73%) emboli were detected on 3D-GRE and 131 (53.7%) emboli were detected on SSFP.

Per-patient basis analysis

The sensitivity, specificity, PPV, NPV, and accuracy of SSFP *vs* 3D-GRE MRI on a per-patient basis was 87.9 *vs* 100%, 100 *vs* 90.9%, 100 *vs* 97.1%, 73.3 *vs* 100%, and 90.9 *vs* 97.8%, respectively. There was no significant difference between the two MRI techniques on a per-patient basis (p = 0.16), and the agreement of SSFP and 3D-GRE with CTPA results was excellent (κ = 0.78 and 0.94, respectively). When both MRI techniques were combined to evaluate PE on a per-patient basis, the sensitivity was 100%, the specificity was 90.9%, the PPV was 97.1%, the NPV was 100%, and the accuracy rate was 97.7%.

Per-embolus basis analysis

The sensitivity, specificity, PPV, NPV, and accuracy of SSFP *vs* 3D-GRE MRI on a per-embolus basis was 53.7 *vs* 73%, 99.6 *vs* 99.5%, 97 *vs* 97.3%, 89.7 *vs* 93.7%, and 90.5 *vs* 94.2%, respectively.

Table 2. The diagnostic performance of pulmonary arterial MRI techniques at lobar and segmental artery levels, on per-embolus basis

	SSFP (n = 44)		3B-GRE (n = 44)	
	Lobar	**Segmental**	**Lobar**	**Segmental**
Sensitivity	67.9 (76/112)	41.7 (55/132)	85.7 (96/112)	62.1 (82/132)
Specificity	99.7 (327/328)	99.5 (657/660)	99.7 (327/328)	99.4 (656/660)
PPV	98.7 (76/77)	94.8 (55/58)	99 (96/97)	95.3 (82/86)
NPV	90.1 (327/363)	89.5 (657/734)	95.3 (327/343)	92.9 (656/706)
Accuracy	%91.6 (403/440)	%89.9 (712/792)	%96.1 (423/440)	%93.1 (738/792)

CTPA, computed tomography pulmonary angiography; 3D-GRE, three-dimensional gradient-echo; MRI, magnetic resonance imaging; NPV, negative predictive value; PPV, positive predictive value; SSFP, steady-state free precession.

Table 3. The diagnostic performance of pulmonary arterial MRI techniques at main and lobar pulmonary arteries

	Right main	Right upper lobe	Right middle lobe	Right lower lobe	Left main	Left upper lobe	Lingula	Left lower lobe
SSFP								
Sensitivity	%70 (7/10)	%30 (3/10)	%23 (3/13)	%87.5 (14/16)	%87.5 (7/8)	%66.6 (4/6)	%57.1 (4/7)	%81.3 (13/16)
Specificity	%100	%100	%100	%96.9	1%00	%100	%100	%100
PPV	%100	%100	%100	%94.1	%100	%100	%100	%100
NPV	%91.9	%91.9	%76.1	%93.9	%97.3	%95.6	%90.9	%88.9
3D-GRE								
Sensitivity	%70 (7/10)	%70 (7/10)	%84.6 (11/13)	%87.5 (14/16)	100 (8/8)	%83.3 (5/6)	%85 6/10	%93.8 15/16
Specificity	%100	%100	%100	%100	%100	%100	%100	%100
PPV	%100	%100	%100	%100	%100	%100	%100	%100
NPV	%91.9	%83	%93.9	%93.3	%100	%97.4	%97.5	%96.6

CTPA, computed tomography pulmonary angiography; 3D-GRE, three-dimensional gradient-echo; MRI, magnetic resonance imaging; NPV, negative predictive value; PPV, positive predictive value; SSFP, steady-state free precession.

The contrast-enhanced 3D-GRE sequence had higher sensitivity and accuracy rates in the detection of emboli (p = 0.0001). The diagnostic performance of the contrast-enhanced 3D-GRE was higher compared to the SSFP at segmental and lobar levels (Table 2). When both MRI sequences were combined, the sensitivity to detect emboli was 74.6%, the specificity was 99.4%, the PPV was 96.8%, the NPV was 94.1%, and the accuracy rate was 94.5%.

Using the CTPA as the gold-standard, the highest sensitivity at lobar PAs was found in the right and left lobar PAs (87.5%) for SSFP, and in the left lower lobe PA (93.8%) for contrast-enhanced 3D-GRE sequence. The lowest sensitivity was at the right middle lobe artery (23.3%) for SSFP, and at the right upper lobe PA (70%) for contrast-enhanced 3D-GRE sequence (Table 3). Three patients with isolated segmental PE on CTPA were all (%100) detected by contrast-enhanced 3D-GRE, while only one (33.4%) patient was detected by SSFP sequence.

Evaluation of lower extremity veins

Per-patient basis analysis

Using the contrast-enhanced 3D-GRE MRV, 34 (77.3%) patients were diagnosed with DVT. Of these, 31 (91%) were detected by Doppler ultrasound whereas 29 (85%) were detected by SSFP technique. MRV detected seven patients (15.9%) with DVT who

Figure 2. A 26-year-old man with chest pain and negative CTPA for PE. Axial CTPA (a), axial contrast enhanced 3D-GRE (b) and axial unenhanced SSFP (c) images shows normal pulmonary arteries. Axial (d), coronal (Ee contrast enhanced 3D-GRE and axial unenhanced SSFP (f) images shows filling defect in the enlarged right main iliac vein *(arrows)* consistent with deep venous thrombosis. The clot is extending to inferior vena cava. 3D-GRE, three-dimensional gradient echo; CTPA, CT pulmonary angiography; SSFP, steady-state-free-precession.

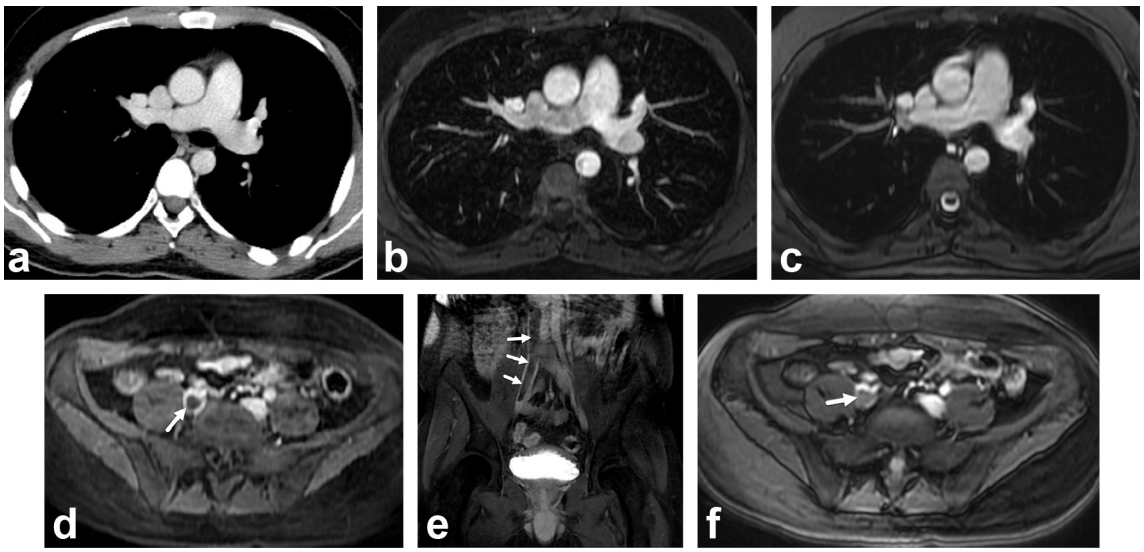

had no PE (Figure 2). Regarding MRV techniques, DVT was evident on both techniques in 29 (66%) patients, however DVT in 5 (11%) patients was detected only on 3D-GRE. The agreement between SSFP and 3D-GRE sequences on a per-patient basis was good (κ = 0.725).

In three patients who had DVT with negative Doppler US, the clot was in the main iliac vein in two of these subjects, and in the distal part of the femoral vein at the adductor canal in one patient. One of the missed thrombi (33%) on Doppler US was detected by SSFP sequence. Associated PE was observed in two of these patients, whereas isolated DVT was seen in one. There were 11 (25%) patients with the diagnosis of DVT in the pelvic (main and external iliac) veins. Two (4.5%) patients had isolated pelvic DVT, whereas nine (20.5%) patients had concomitant thrombi in the other venous segments. Both two patients with isolated pelvic DVT were not diagnosed by Doppler US. However, SSFP showed thrombus in one subject.

Per-thrombus analysis

We evaluated 704 venous segments in 44 patients and there was thrombus in 110 (15.6%) segments on 3D-GRE MRV. Doppler US detected thrombus is 92 (13%) segments and SSFP detected thrombus in 93 segments (13.2%). The most frequent location for thrombus was left popliteal vein seen in 14 (32%) patients. In comparison of Doppler US and SSFP sequence on a per-thrombus basis, the clot was detected in 81 (11.5%) segments by both imaging techniques, whereas the thrombus was evident only on SSFP in 12 (1.7%) segments, and only on Doppler US in 11 (1.6%) segments. The agreement between SSFP and Doppler US was excellent on a per-thrombus basis (κ = 0.857). In comparison of Doppler US and 3D-GRE there was an excellent agreement (κ = 0.896). In comparison of SSFP and 3D-GRE techniques on a per-thrombus basis, the thrombus was detected in 93 (13.2%) segments by both techniques, whereas it was detected only by 3D-GRE sequence in 17 (2.4%) segments (κ = 0.902).

We evaluated 176 pelvic (the main and external iliac) venous segments in 44 patients; of 88 main iliac veins, there was thrombus in 8 (9.1%) segments on 3D-GRE. However, no thrombus was detected by Doppler ultrasonography while SSFP detected DVT in six (6.8%) segments. Regarding external iliac veins, thrombus was detected in 18 (10.2%) segments on 3D-GRE. However, Doppler ultrasonography detected DVT in 3 (1.7%) segments and SSFP identified DVT in 13 (7.4%) segments.

DISCUSSION

Our study shows that unenhanced or contrast-enhanced combined pulmonary MRI and MRV is a feasible one-stop-shopping technique in patients with suspected VTE. Using CTPA as a gold-standard, the sensitivity of pulmonary MRI has been determined as 100% for the contrast-enhanced 3D-GRE technique and 87.9% for unenhanced SSFP on a per-patient basis. Unenhanced lower extremity MRV is also successful and performed better than Doppler US for the diagnosis of DVT and agreement between unenhanced SSFP and contrast-enhanced 3D-GRE techniques was excellent on a per-thrombus basis (κ = 0.902).

Although CTPA has become the front-line imaging modality with good accuracy rates in the diagnosis of PE,[10,11] concerns about ionizing radiation and the risks of contrast material remain increased.[12] These concerns are particularly important in pregnant patients in whom the risk of VTE is increased. Previous studies comparing CTPA and MRI techniques in the diagnosis of PE reported promising results. Cronin and Dwamena[13] recently reported that the use of contrast-enhanced MR angiography for the diagnosis of PE had a higher positive likelihood ratio than CTPA. They[13] have used the PIOPED II and PIOPED III data to calculate (likelihood ratio) for PE in their cohort based on the pre-test probability from clinical prediction rules (*i.e.* Wells score, Geneva score, Miniati score, and Charlotte score). A recent meta-analysis, which includes 15 studies, showed that MRI had an overall sensitivity of 75% and specificity of 80% in the diagnosis of PE on a patient-based analysis.[14] On a vessel basis, the pooled sensitivity and specificity of five studies with technically adequate image quality were 84 and 98% respectively.[14] In a recent study, Nyrén et al[15] compared CTPA and repeated acquisitions of MRI using SSFP sequence and they reported a sensitivity of SSFP sequence 90–93% (for Observer 1 and 2) and specificity of 100% (for both observers). In our study, the sensitivity and specificity of SSFP *vs* 3D-GRE were 88 *vs* 100 and 100 *vs* 91%, respectively on a per-patient basis. The diagnostic performance of both techniques was lower on per-embolus basis. This finding is in concordance with the study by Kalb et al[16] who compared three different MRI techniques (MRA, SSFP, 3D-GRE) with CTPA. Our study differs from the similarly designed study of Kalb et al,[16] as they only included patients with known PE. However, we randomly included patients without knowing the results of CTPA who had a suspicion of PE and participate to our study.

The diagnostic accuracy of MRI techniques is high in large vessels. In PIOPED III[17] study, the sensitivity of MRA in the diagnosis PE in patients with good image quality was 79% in the main and lobar levels, and 50% in the segmental level. Revel et al[18] compared CTPA and MRI in the diagnosis of PE in 274 patients by two different readers. CTPA detected a total of 103 emboli, and the sensitivity of SSFP and MRA at lobar PAs for both readers was 100% whereas this figure was 82.3% (SSFP) and 86.4% (MRA) for the first reader in the segmental level, and 50% (SSFP) and 81.8% (MRA) for the second reader. Zhang et al[19] compared CTPA and 3 T MRA techniques and reported a sensitivity of 100 and 65.2% at the level of lobar and segmental PAs, respectively. Schiebler et al[20] reported MRA has a NPV of 99% (95%CI: 97–100%) in 500 patients with suspected PE. In our study, the sensitivities for SSFP and 3D-GRE sequences respectively were 67.9 and 85.7% at the lobar PAs level, and 41.7 and 62.1% at the segmental PAs level. When two MRI techniques (SSFP, 3D-GRE) were combined to evaluate the emboli on a per-patient and per-embolus basis, the sensitivities were 100 and 75%, the specificities were 91%, 97%, and the accuracy rates were 98 and 95%, respectively. The slightly lower sensitivity rates in our study, especially in the SSFP sequence, can be explained by the larger slice thickness (5 mm in SSFP) used in our study while it was 3–4 mm in

similar studies.[16,18,19] We also did not employ respiratory or ECG gating in our study which could minimize the motion artifacts and improve the image quality.[16,18]

The image quality affects the diagnostic performance of MRI techniques in the assessment of PE. In PIOPED III study, 25% technically limited image was reported.[17] A meta-analysis of 15 studies showed that MRI was technically inadequate in 2–28% of patients.[14] In a recent report, authors found that the rate of technically "limited" contrast-enhanced MR angiography images was 8.8%.[20] In line with the recent literature, we found the image quality of the pulmonary MRI was rated as limited in 2 and 7% of subjects on SSFP and 3D-GRE techniques, respectively. The sensitivity increased from 54 to 61% for SSFP, and from 73 to 81% for 3D-GRE on per-embolus basis in patients with adequate image quality. Optimized imaging techniques in a cooperative patient would likely to result in improved image quality and better diagnostic performance.

The anatomical location of the embolus may cause difficulty in detection. This is particularly prominent in the lingula and the right middle lobe arteries where motion artifacts due to heart motion are more pronounced.[16–19,21–25] In line with the literature, we found the lowest sensitivity (23%) at the right middle lobe artery on SSFP sequence, and the highest sensitivity at the right lower lobe (87.5% on SSFP and 87.5% on 3D-GRE) and left lower lobe arteries (81.3% on SSFP and 93.8% on 3D-GRE). Kalb et al[16] reported the lowest sensitivity in detecting PE in the lingual (43%) and demonstrated that the motion artifacts from cardiac and respiratory motion were the most commonly observed imaging problem. The severity of PE is related to its location, and the risk is higher in central emboli.[26] Isolated subsegmental PE is observed at a rate of 4–6% in clinically suspected PE cases[27–29] with controversial clinical impact.[28,29] The sensitivity of pulmonary arterial MRI in detecting segmental–subsegmental embolism is low.[16,18,19,30–33] In line with literature, in our study, of overall 132 segmental emboli seen on CTPA, 48 (36%) emboli could not be detected on any of pulmonary arterial MRI techniques.

False-positive results in patients with suspected PE may lead to unnecessary intervention. In the evaluation of three different MRI techniques (MRA, SSFP and 3D-GRE), Kalb et al[16] reported only one (2.6%) false-positive result in MRA in 22 patients with PE. Zhang et al[19] reported no false-positivity for the first reader whereas five (10%) false-positive results were reported for the second reader in the lobar and segmental PAs. In a larger series encompassing 118 patients, Ouderk et al[23] reported false-positivity on the MRA in 2 (7%) patients. Kluge et al[22] reported 27 (16%) and 3 (10%) false-positive results at segmental and lobar levels, respectively using MRA. In our study, we found 0.9% (1/112) false-positive at the lobar, and 2.3% (3/132) false-positive results at segmental levels, respectively in SSFP, whereas one (0.9%) at lobar, and four (3%) false-positive results at segmental levels, respectively on 3D-GRE. Motion artifacts due to the heart beat and respiration and inadequate contrast were the leading causes of false positivity.[34] The use of cardiac and respiratory gating could have minimized the motion artifacts and decreased false-positive rate.

Imaging of the lower extremity veins in patients with suspected PE is important for the evaluation of potential culprit thrombi. Doppler ultrasonography has been used as the first-line modality for this purpose. However, the sensitivity of Doppler ultrasonography at the thigh and pelvic region is low.[35–38] MRV of the lower extremities has also been recommended for the assessment of DVT in patients with suspected PTE.[7,9,39] Using CE-venography as the gold-standard in a meta-analysis, the pooled sensitivity and specificity of MRV as 91.5 and 94.8%, respectively.[40] A recent meta-analysis by Abdalla et al[41] also showed that the pooled sensitivity and specificity of lower extremity MRV was 93 and 96%, respectively. Kluge et al[9] reported superior performance of contrast-enhanced indirect MRV compared to Doppler ultrasonography in DVT detection. We also compared unenhanced, contrast-enhanced MRV techniques and Doppler ultrasonography in DVT detection. When we used contrast-enhanced 3D-GRE technique as a gold-standard in DVT detection there was an excellent agreement between 3D-GRE and SSFP techniques ($\kappa = 0.902$) per-thrombus bases and there was superior performance of unenhanced MRV compared to Doppler US in DVT detection. Although no previous study compared unenhanced and contrast-enhanced MRV techniques in the setting of VTE, the better performance of the enhanced 3D-GRE MRV in our study is plausible due to enhancing effect of the contrast material. In our study, MRV detected seven (15.9%) patients with DVT who had no PE on CTPA. Thus, the addition of MRV increased the VTE rate by 17.5% (7/40). This finding is supported by CT data in which the addition of indirect CT venography in routine CTPA protocols has been proved to increase the rate of VTE diagnosis by 14 to 27%.[42–44] Similarly, the sensitivity of combined pulmonary MRA and MRV in detecting VTE increased from 78 to 92% in the PIOPED III.[17] Kluge et al[9] also reported a 17% increase in VTE by the addition of indirect MRV.

There were some limitations in our study. First, our study population is small and the number of patients with PE was higher than those without PE. This disproportion may be due to patients with severe clinical symptoms are more likely to participate in the study. Second, since the images were evaluated by single radiologist, we did not assess interobserver variability. Third, we did not use the respiratory or cardiac gating that would have minimized the motion artifact and potentially improved diagnostic performance. Fourth, we used thicker slices in SSFP compared to contrast-enhanced 3D-GRE technique. Thinner slices may have provided higher spatial resolution at the expense of longer imaging time. Fifth, we used indirect contrast-enhanced MRV as the gold-standard method for DVT diagnosis. Contrast venography is the gold-standard for the diagnosis of DVT, but it is invasive tool and includes radiation exposure. Also, a recent meta-analysis of 16 studies showed that the pooled sensitivity and specificity of lower extremity MRV was 93 and 96%, respectively.[41] Finally, as the time interval between CTPA and MRI was 26.6 ± 22.4 h (range: 1–72 h) in our study, some PE might have disappeared at the time of MRI.

In conclusion, combined MRI (chest MRI and lower extremity MRV) is a feasible one-stop-shopping technique in patients with suspected thromboembolism. This technique may be considered as an alternative modality in patients who have contraindications to CTPA. Although the contrast-enhanced 3D-GRE performs better than unenhanced SSFP in the detection of PE, the latter can be used as a primary comprehensive technique in VTE detection in patients with contraindications to gadolinium-based contrast agents such as pregnant subjects and those with renal insufficiency.

REFERENCES

1. Jaff MR, McMurtry MS, Archer SL, Cushman M, Goldenberg N, Goldhaber SZ, et al. Management of massive and submassive pulmonary embolism, iliofemoral deep vein thrombosis, and chronic thromboembolic pulmonary hypertension: a scientific statement from the American Heart Association. *Circulation* 2011; **123**: 1788–830. doi: https://doi.org/10.1161/CIR.0b013e318214914f
2. Righini M, Le Gal G, Aujesky D, Roy P-M, Sanchez O, Verschuren F, et al. Diagnosis of pulmonary embolism by multidetector CT alone or combined with venous ultrasonography of the leg: a randomised non-inferiority trial. *The Lancet* 2008; **371**: 1343–52. doi: https://doi.org/10.1016/S0140-6736(08)60594-2
3. Da Costa Rodrigues J, Alzuphar S, Combescure C, Le Gal G, Perrier A. Diagnostic characteristics of lower limb venous compression ultrasonography in suspected pulmonary embolism: a meta-analysis. *J Thromb Haemost* 2016; **14**: 1765–72. doi: https://doi.org/10.1111/jth.13407
4. Torbicki A, Perrier A, Konstantinides S, Agnelli G, Galiè N, Pruszczyk P, et al. Guidelines on the diagnosis and management of acute pulmonary embolism: the task Force for the diagnosis and management of acute pulmonary embolism of the European Society of cardiology (ESC). *Eur Heart J* 2008; **29**: 2276–315. doi: https://doi.org/10.1093/eurheartj/ehn310
5. Karande GY, Hedgire SS, Sanchez Y, Baliyan V, Mishra V, Ganguli S, et al. Advanced imaging in acute and chronic deep vein thrombosis. *Cardiovasc Diagn Ther* 2016; **6**: 493–507. doi: https://doi.org/10.21037/cdt.2016.12.06
6. Tsuchiya N, van Beek EJ, Ohno Y, Hatabu H, Kauczor HU, Swift A, et al. Magnetic resonance angiography for the primary diagnosis of pulmonary embolism: a review from the International workshop for pulmonary functional imaging. *World J Radiol* 2018; **10**: 52–64. doi: https://doi.org/10.4329/wjr.v10.i6.52
7. Cantwell CP, Cradock A, Bruzzi J, Fitzpatrick P, Eustace S, Murray JG. MR venography with true fast imaging with steady-state precession for suspected lower-limb deep vein thrombosis. *J Vasc Interv Radiol* 2006; **17**(11 Pt 1): 1763–70. doi: https://doi.org/10.1097/01.RVI.0000242502.40626.53
8. Hadizadeh DR, Kukuk GM, Fahlenkamp UL, Pressacco J, Schäfer C, Rabe E, et al. Simultaneous Mr arteriography and venography with blood pool contrast agent detects deep venous thrombosis in suspected arterial disease. *AJR Am J Roentgenol* 2012; **198**: 1188–95. doi: https://doi.org/10.2214/AJR.11.7306
9. Kluge A, Mueller C, Strunk J, Lange U, Bachmann G. Experience in 207 combined MRI examinations for acute pulmonary embolism and *deep vein thrombosis*. *AJR Am J Roentgenol* 2006; **186**: 1686–96. doi: https://doi.org/10.2214/AJR.05.0756
10. Remy-Jardin M, Pistolesi M, Goodman LR, Gefter WB, Gottschalk A, Mayo JR, et al. Management of suspected acute pulmonary embolism in the era of CT angiography: a statement from the Fleischner Society. *Radiology* 2007; **245**: 315–29. doi: https://doi.org/10.1148/radiol.2452070397
11. Stein PD, Fowler SE, Goodman LR, Gottschalk A, Hales CA, Hull RD, et al. Multidetector computed tomography for acute pulmonary embolism. *N Engl J Med* 2006; **354**: 2317–27. doi: https://doi.org/10.1056/NEJMoa052367
12. Mitchell AM, Kline JA. Contrast nephropathy following computed tomography angiography of the chest for pulmonary embolism in the emergency department. *J Thromb Haemost* 2007; **5**: 50–4. doi: https://doi.org/10.1111/j.1538-7836.2006.02251.x
13. Cronin P, Dwamena BA. A clinically meaningful interpretation of the prospective investigation of pulmonary embolism diagnosis (PIOPED) II and III data. *Acad Radiol* 2018; **25**: 561–72. doi: https://doi.org/10.1016/j.acra.2017.11.014
14. Zhou M, Hu Y, Long X, Liu D, Liu L, Dong C, et al. Diagnostic performance of magnetic resonance imaging for acute pulmonary embolism: a systematic review and meta-analysis. *J Thromb Haemost* 2015; **13**: 1623–34. doi: https://doi.org/10.1111/jth.13054
15. Nyrén S, Nordgren Rogberg A, Vargas Paris R, Bengtsson B, Westerlund E, Lindholm P. Detection of pulmonary embolism using repeated MRI acquisitions without respiratory gating: a preliminary study. *Acta Radiol* 2017; **58**: 272–8. doi: https://doi.org/10.1177/0284185116651003
16. Kalb B, Sharma P, Tigges S, Ray GL, Kitajima HD, Costello JR, et al. MR imaging of pulmonary embolism: diagnostic accuracy of contrast-enhanced 3D Mr pulmonary angiography, contrast-enhanced low-flip angle 3D GRE, and nonenhanced free-induction FISP sequences. *Radiology* 2012; **263**: 271–8. doi: https://doi.org/10.1148/radiol.12110224
17. Stein PD, Chenevert TL, Fowler SE, Goodman LR, Gottschalk A, Hales CA, et al. Gadolinium-enhanced magnetic resonance angiography for pulmonary embolism: a multicenter prospective study (PIOPED III. *Ann Intern Med* 2010; **152**: 434–43. doi: https://doi.org/10.7326/0003-4819-152-7-201004060-00008
18. Revel MP, Sanchez O, Lefort C, Meyer G, Couchon S, Hernigou A, et al. Diagnostic accuracy of unenhanced, contrast-enhanced perfusion and angiographic MRI sequences for pulmonary embolism diagnosis: results of independent sequence readings. *Eur Radiol* 2013; **23**: 2374–82. doi: https://doi.org/10.1007/s00330-013-2852-8
19. Zhang LJ, Luo S, Yeh BM, Zhou CS, Tang CX, Zhao Y, et al. Diagnostic accuracy of three-dimensional contrast-enhanced MR angiography at 3-T for acute pulmonary embolism detection: comparison with multidetector CT angiography. *Int J Cardiol* 2013; **168**: 4775–83. doi: https://doi.org/10.1016/j.ijcard.2013.07.228
20. Schiebler M, Francois C, Repplinger M, Hamedani A, Lindholm C, Vigen K. Effectiveness of pulmonary contrast enhanced magnetic Resonance angiography for the primary workup of pulmonary

embolism. *ISMRM 24th Annual Meeting and Exhibition* 2016;.
21. Nagle SK, Schiebler ML, Repplinger MD, François CJ, Vigen KK, Yarlagadda R, et al. Contrast enhanced pulmonary magnetic resonance angiography for pulmonary embolism: building a successful program. *Eur J Radiol* 2016; **85**: 553–63. doi: https://doi.org/10.1016/j.ejrad.2015.12.018
22. Kluge A, Luboldt W, Bachmann G. Acute pulmonary embolism to the subsegmental level: diagnostic accuracy of three MRI techniques compared with 16-MDCT. *AJR Am J Roentgenol* 2006; **187**: W7–W14. doi: https://doi.org/10.2214/AJR.04.1814
23. Oudkerk M, van Beek EJR, Wielopolski P, van Ooijen PMA, Brouwers-Kuyper EMJ, Bongaerts AHH, et al. Comparison of contrast-enhanced magnetic resonance angiography and conventional pulmonary angiography for the diagnosis of pulmonary embolism: a prospective study. *The Lancet* 2002; **359**: 1643–7. doi: https://doi.org/10.1016/S0140-6736(02)08596-3
24. Kang MJ, Park CM, Lee CH, Goo JM, Lee HJ. Focal iodine defects on color-coded iodine perfusion maps of dual-energy pulmonary CT angiography images: a potential diagnostic pitfall. *AJR Am J Roentgenol* 2010; **195**: W325–W330. doi: https://doi.org/10.2214/AJR.09.3241
25. Sohns C, Amarteifio E, Sossalla S, Heuser M, Obenauer S. 64-Multidetector-row spiral CT in pulmonary embolism with emphasis on incidental findings. *Clin Imaging* 2008; **32**: 335–41. doi: https://doi.org/10.1016/j.clinimag.2008.01.028
26. Ghanima W, Abdelnoor M, Holmen LO, Nielssen BE, Sandset PM. The association between the proximal extension of the clot and the severity of pulmonary embolism (PE): a proposal for a new radiological score for PE. *J Intern Med* 2007; **261**: 74–81. doi: https://doi.org/10.1111/j.1365-2796.2006.01733.x
27. .PIOPED Investigators Value of the ventilation/perfusion scan in acute pulmonary embolism. Results of the prospective investigation of pulmonary embolism diagnosis (PIOPED. *JAMA* 1990; **263**: 2753–9.
28. Stein PD, Henry JW, Gottschalk A. Reassessment of pulmonary angiography for the diagnosis of pulmonary embolism: relation of interpreter agreement to the order of the involved pulmonary arterial branch. *Radiology* 1999; **210**: 689–91. doi: https://doi.org/10.1148/radiology.210.3.r99mr41689
29. Carrier M, Klok FA. Symptomatic subsegmental pulmonary embolism: to treat or not to treat? *Hematology Am Soc Hematol Educ Program* 2017; **2017**: 237–41. doi: https://doi.org/10.1182/asheducation-2017.1.237
30. Kluge A, Mueller C, Strunk J, Lange U, Bachmann G. Experience in 207 combined MRI examinations for acute pulmonary embolism and *deep vein thrombosis*. *AJR Am J Roentgenol* 2006; **186**: 1686–96. doi: https://doi.org/10.2214/AJR.05.0756
31. Ohno Y, Higashino T, Takenaka D, Sugimoto K, Yoshikawa T, Kawai H, et al. MR angiography with sensitivity encoding (sense) for suspected pulmonary embolism: comparison with MDCT and ventilation-perfusion scintigraphy. *AJR Am J Roentgenol* 2004; **183**: 91–8. doi: https://doi.org/10.2214/ajr.183.1.1830091
32. Nael K, Michaely HJ, Kramer U, Lee MH, Goldin J, Laub G, et al. Pulmonary circulation: contrast-enhanced 3.0-T MR angiography--initial results. *Radiology* 2006; **240**: 858–68. doi: https://doi.org/10.1148/radiol.2403051076
33. Herédia V, Altun E, Ramalho M, de Campos R, Azevedo R, Pamuklar E, et al. MRI of pregnant patients for suspected pulmonary embolism: steady-state free precession vs postgadolinium 3D-GRE. *Acta Med Port* 2012; **25**: 359–67.
34. Benson DG, Schiebler ML, Repplinger MD, François CJ, Grist TM, Reeder SB, et al. Contrast-enhanced pulmonary MRA for the primary diagnosis of pulmonary embolism: current state of the art and future directions. *Br J Radiol* 2017; **90**: 20160901. doi: https://doi.org/10.1259/bjr.20160901
35. Lewis BD. The peripheral veins. In: ultrasound D, ed. *Bumack CM, Wilson SR, Charboneau JW*. 3rd ed. St. Louis: Mo: Elsevier Mosby; 2005. pp. 1019–35.
36. Spritzer CE, Arata MA, Freed KS. Isolated pelvic deep venous thrombosis: Relative frequency as detected with MR imaging. *Radiology* 2001; **219**: 521–5. doi: https://doi.org/10.1148/radiology.219.2.r01ma25521
37. Hansch A, Betge S, Poehlmann G, Neumann S, Baltzer P, Pfeil A, et al. Combined magnetic resonance imaging of deep venous thrombosis and pulmonary arteries after a single injection of a blood pool contrast agent. *Eur Radiol* 2011; **21**: 318–25. doi: https://doi.org/10.1007/s00330-010-1918-0
38. Lindquist CM, Karlicki F, Lawrence P, Strzelczyk J, Pawlyshyn N, Kirkpatrick IDC. Utility of balanced steady-state free precession MR venography in the diagnosis of lower extremity deep venous thrombosis. *American Journal of Roentgenology* 2010; **194**: 1357–64. doi: https://doi.org/10.2214/AJR.09.3552
39. Ohno Y, Yoshikawa T, Kishida Y, Seki S, Karabulut N, Unenhanced KN. Unenhanced and contrast-enhanced MR angiography and perfusion imaging for suspected pulmonary thromboembolism. *AJR Am J Roentgenol* 2017; **208**: 517–30. doi: https://doi.org/10.2214/AJR.16.17415
40. Sampson FC, Goodacre SW, Thomas SM, van Beek EJ. The accuracy of MRI in diagnosis of suspected deep vein thrombosis: systematic review and meta-analysis. *Eur Radiol* 2007; **17**: 175–81. doi: https://doi.org/10.1007/s00330-006-0178-5
41. Abdalla G, Fawzi Matuk R, Venugopal V, Verde F, Magnuson TH, Schweitzer MA, et al. The diagnostic accuracy of magnetic resonance venography in the detection of deep venous thrombosis: a systematic review and meta-analysis. *Clin Radiol* 2015; **70**: 858–71. doi: https://doi.org/10.1016/j.crad.2015.04.007
42. Loud PA, Katz DS, Bruce DA, Klippenstein DL, Grossman ZD. Deep venous thrombosis with suspected pulmonary embolism: detection with combined CT venography and pulmonary angiography. *Radiology* 2001; **219**: 498–502. doi: https://doi.org/10.1148/radiology.219.2.r01ma26498
43. Cham MD, Yankelevitz DF, Shaham D, Shah AA, Sherman L, Lewis A, et al. Deep venous thrombosis: detection by using indirect CT venography. the pulmonary Angiography-Indirect CT venography Cooperative Group. *Radiology* 2000; **216**: 744–51. doi: https://doi.org/10.1148/radiology.216.3.r00se44744
44. Ghaye B, Nchimi A, Noukoua CT, Dondelinger RF. Does multi-detector row CT pulmonary angiography reduce the incremental value of indirect CT venography compared with single-detector row CT pulmonary angiography? *Radiology* 2006; **240**: 256–62. doi: https://doi.org/10.1148/radiol.2401050350